Results in Physics 2 (2012) 58–65

Contents lists available at SciVerse ScienceDirect

Results in Physics

journal homepage: www.elsevier.com/locate/rinp

# Structural and electronic properties of the Laves phase based on rare earth type $BaM_2$ (M = Rh, Pd, Pt)

A. Yakoubi [a,*], O. Baraka [b], B. Bouhafs [a]

[a] Modeling and Simulation in Materials Science Laboratory, Physics Department, University of Sidi Bel-Abbes, Sidi Bel-Abbes, Algeria
[b] Département de Physique, Faculté des Sciences, Université Djillali Liabès, Sidi-Bel-Abbès, Algeria

ARTICLE INFO

*Article history:*
Received 2 May 2012
Accepted 5 June 2012
Available online 13 June 2012

*Keywords:*
Density functional theory
Crystal structure
Laves phase
Elastic properties

ABSTRACT

We will presented the study of structural, electronic and elastic properties of Laves phase based on rare earth type $BaM_2$ (M = Rh, Pd, Pt). For this, we used the method of linear augmented plane wave (FP-LAPW) based on density functional theory (DFT).

We studied the structural properties, we calculated the formation energy to prove the existence of these compounds experimentally and the cohesive energy to determine the energy required to disassemble into its component parts, then the electronic properties. And finally, we calculated the elastic constants.



## 1. Introduction

Binary Laves phases $AB_2$ is a rich family of intermetallic compounds. A is an electropositive element such as an alkali metal, an alkaline earth metal, a lanthanide, an actinide or transition element groups IIIB and IVB. When for B, it is a transition element less electropositive than A, for example, metals from groups VIIB and VIIIB or a noble metal. These systems crystallize in three structures: hexagonal or C14, face centered cubic or C15 (majority) and dihexagonal C36 (minority). These compounds were discovered in 1927 by James Friauf [1]. Fritz Laves structures studied exhaustively in the 30's [2]. Their names derive of the names of these two researchers, "Friauf Laves phases" or generally "Laves phases". These phases are characterized by a mixture ratio of two specific metal elements, which distinguishes them from conventionals metals intermetallics. They are compact ordered structures with the chemical formula $AB_2$ for the stoichiometric compound and an ideal ratio of radii $r_A/r_B$ around $(3/2)^{1/2}$.

The ground-state properties of Laves phases $AB_2$ (A stands for transition metals or rare earth elements, and B stands for transition metals) compounds are of considerable scientific and technological interests, and have been the subject of many investigations during the last decade [3] because these Laves phases show remarkable mechanical and physical properties [4]. These phases have quite high melting temperatures, low densities, and high oxidation resistances, which are necessary for high-temperature structural applications. Current research is centered on the use of fine precipitates of Laves phases on turbine steels to improve their fatigue strength [5]. Some binary intermetallic $AB_2$ have unique magnetic properties and superconducting [6,7]. At present, interests have been focused on the development of hydrogen-storage materials [8,9], and the class of Laves phases compounds with C15 crystal structure is a promising candidate [10].

The structure of C15 is a face-centered cubic structure defined in the space group Fd-3 m (N° 227) in Hermann–Mauguin notation; it contains eight formula units (f.u) in the conventional cell, or two f.u in the primitive cell because the space group behind the F mode ($Z = 4$). There are therefore a total of 24 atoms per cell; the crystal structure of the archetype of $MgCu_2$ C15 compounds is comparable to that of diamond because the atoms of the subnet A (= Mg) are organized as the carbon atoms of the diamond cubic; the atoms of subnet B (= Cu) form tetrahedra which share two to two the tops.

We apply density functional theory with a plane-wave basis for understand the behavior of electronic structures, mechanical properties and bonding characteristic of Laves phases on rare earth types $BaM_2$ (M = Rh, Pd, Pt) with the cubic structure C15 prototype $MgCu_2$ [11]. Using first principles calculations, a fundamental understanding of the electronic and mechanical properties of $BaM_2$ (M = Rh, Pd, Pt) Laves phases is of paramount importance, because such an understanding is essential for deriving the scientific principles to improve their physical and mechanical properties and for broadening the potential structural applications of these compounds and to account for the electronic and magnetic structures not accessible by experiment relatively favorable.

* Corresponding author.
*E-mail address:* yakoubi_aek@yahoo.fr (A. Yakoubi).

2211-3797 
http://dx.doi.org/10.1016/j.rinp.2012.06.001

In this paper, the lattice constants, formation and cohesive energy, energy bands, total density of states (DOS), bonding charge densities and elastic constants of $BaM_2$ (M = Rh, Pd, Pt) were calculated using first principles are analyzed and discussed.

## 2. Calculation method

Currently, there are different codes of theoretical calculations with different approximations. In our calculations, we use the Wien2k [12] which is a direct application of the FP-LAPW developed by Blaha et al. [13], will allow us to study the structural, electronic and elastic properties of Laves phases based on rare-earth types $BaM_2$ or M = Rh, Pd, Pt using the Bravais lattice and space group symmetry.

The algorithm is based on the density functional theory (DFT) within the local density approximation (LDA) proposed by Perdew and Wang [14] for the exchange correlations functional. It calculates the self-consistent solution of the equations of Kohn and Sham [15] who decry the valence electron in a potential created by a periodic array. The basis functions, the electron densities and the potentials are in combination of spherical harmonics around the atomic sites, i.e. atomic spheres, with a cutoff $l_{max} = 10$, and Fourier series in the interstitial region. To obtain the convergence of proper value, the wave functions in the interstitial region are expanded in plane waves with a cutoff of $R_{MT} \times K_{max}$ equal to 9 (where $R_{MT}$ is the average radius of the muffin-tin spheres and $K_{max}$ is the maximum value of the wave vector $K = k + G$).

In these calculations, the energy separation is −6.0 Ry for all compounds, was used between the valence states and the core states. The choice of muffin-tin (MT) radii for the various atoms in the crystal show small differences that do not affect our results. We have adopted the value of 2.5 Bohr for atomic spheres barium (Ba) and 2.3 Bohr for atomic spheres rhodium (Rh), palladium (Pd) and platinum (Pt). The electronic configurations for Ba, Rh, Pd and Pt are Ba: [Xe] $6s^2$, Rh: [Kr] $4d^8$ $5s^1$, Pd: [Kr] $4d^{10}$ and Pt: [Xe] $4f^{14}$ $5d^9$ $6s^1$. In the calculation, the subshells of the noble gas cores have been distinguished from the subshells of valence electrons given explicitly.

We also mention that the integration in reciprocal lattice space as performed using the special point's method. We use a $14 \times 14 \times 14$ mesh (104 k-points) for our structure. The $k$ integration over the Brillouin zone is performed using the Monkhorst and Pack mesh [16].

## 3. Results and discussions

### 3.1. Structural properties

#### 3.1.1. Lattice parameters and bulk modulus

$BaRh_2$, $BaPd_2$ and $BaPt_2$ like most of the Laves phases are of $AB_2$ stoichiometry with space group Fd-3m and crystallize in the $MgCu_2$ crystal structure and whose atoms occupy the Wyckoff positions 2(a) [(1/8,1/8,1/8), (7/8,7/8,7/8)] for Ba, and 16(d) [(1/2,1/2,1/2), (1/2,3/4,3/4), (3/4,1/2,3/4), (3/4,3/4,1/2)] for Rh, Pd and Pt (see example on Fig. 1) [17]. We have used the experiment lattice constant to start calculations. We then vary these parameters until reaching the minimum of energy. We have therefore performed detailed structural optimizations of the unit cell geometries as a function of the external stress by minimizing the total energy. In Table 1, we summarize our calculated structural properties (lattice constant, bulk modulus and its pressure derivative) of $BaRh_2$, $BaPd_2$ and $BaPt_2$ with the LDA.

The lattice constants and bulk modulus are computed by fitting the total energy versus volume according to the Murnaghan's equation of state [18].

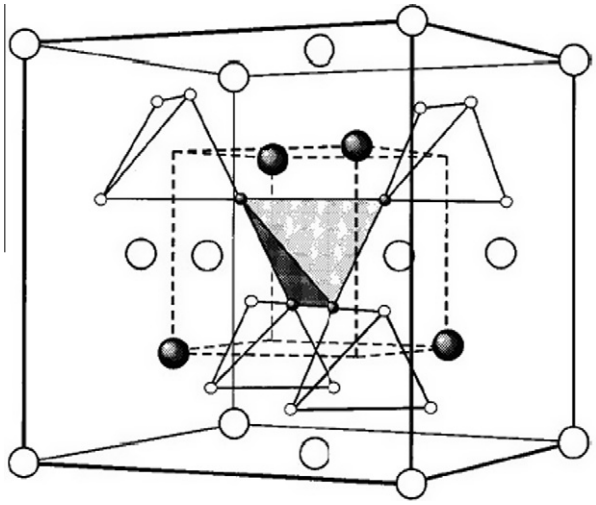

**Fig. 1.** Crystal structure of cubic binary $AB_2$ Laves phase compounds. Small symbols represent the B atom positions whereas the large ones represent the A atoms. Broken lines indicate the primitive cell, which contains two formula units (shaded symbols).

**Table 1**
The calculated lattice constants, bulk modulus ($B$), bulk modulus's pressure derivatives ($B'$), energy of formation ($E_{for}$) and cohesive energy ($E_{coh}$) of the C15-$BaM_2$.

| | Lattice (Å) | $B$ (GPa) | $B'$ | $E_{for}$ (eV/atom) | $E_{coh}$ (eV/atom) |
|---|---|---|---|---|---|
| $BaRh_2$ | 7.717<br>7.852[a] | 127.42 | 4.06 | −0.107 | 6.101 |
| $BaPd_2$ | 7.837<br>7.953[a] | 107.81 | 4.12 | −0.660 | 4.774 |
| $BaPt_2$ | 7.853<br>7.920[a] | 140.69 | 4.32 | −0.823 | 6.512 |

[a] Experement by XRD [19].

When we analyze our results we found that there is good agreement between our results and experimental data, In comparison with the experimental data we found that LDA underestimate the lattice constant compared to the experimental values (commonly observed) by 1.72%, 1.46% and 0.85% for $BaRh_2$, $BaPd_2$ and $BaPt_2$, respectively.

The bulk modulus B is computed to be 127.42 GPa, 107.81 GPa and 140.69 GPa for $BaRh_2$, $BaPd_2$ and $BaPt_2$, respectively.

#### 3.1.2. Formation and cohesive energy

To study the relative phase stabilities, we have calculated the energy of formation for $BaM_2$. The energy of formation per atom is defined as [20]:

$$E_{form}^{BaM_2} = \frac{E_{total}^{BaM_2} - xE_{solid}^{Ba} - yE_{solid}^{M}}{x+y} \Rightarrow E_{form}^{BaM_2} = \frac{E_{total}^{BaM_2} - 2E_{solid}^{Ba} - 4E_{solid}^{M}}{6} \quad (\text{with M} = \text{Rh, Pd, Pt.}) \tag{1}$$

where $x$ and $y$ are the numbers of Ba and (Rh, Pd, Pt) atoms in unit cell, respectively. $E_{total}^{BaM_2}$, $E_{solid}^{Ba}$ and $E_{solid}^{M}$ are the calculated total energies of the C15-type $BaM_2$ compounds, Ba, and M, respectively. During calculation, Ba and M are taken as body-centered cubic structure (space group Im-3m) and cubic close-packed (space group Fm-3m), respectively. The calculation of formation energies are presented in Table 1.

The calculation of the formation energy gives the following values −0.107 eV/atom, −0.660 eV/atom and −0.823 eV/atom for $BaRh_2$, $BaPd_2$ and $BaPt_2$, respectively, which are all negative. Such a negative value of $E_{for}$ implies that the $BaM_2$ phases are energeti-

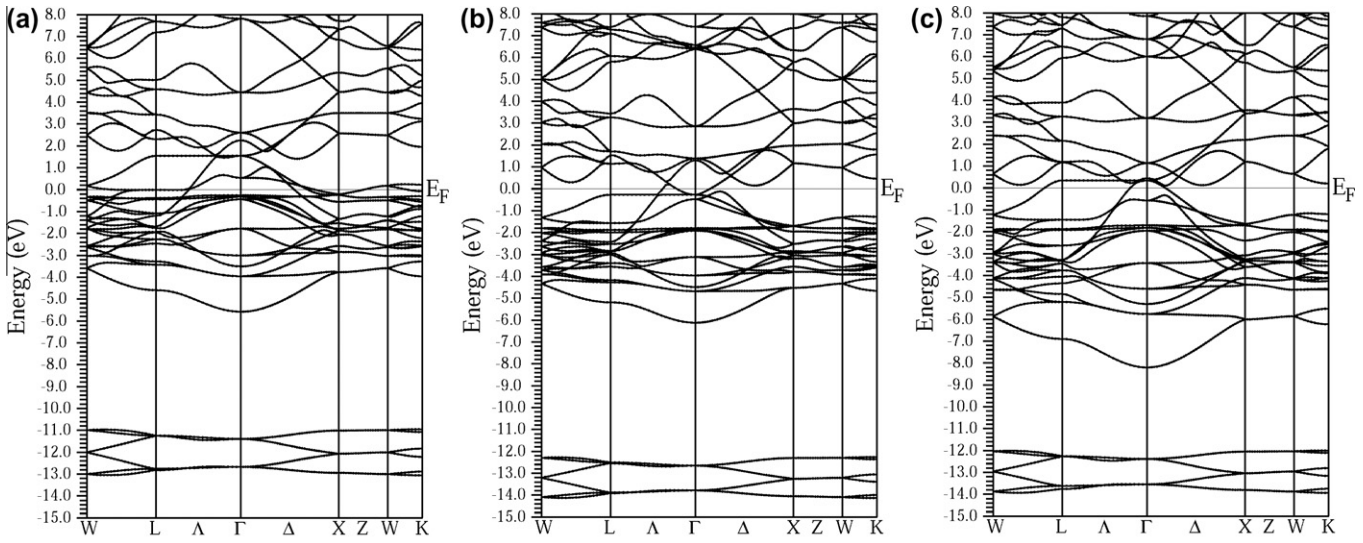


**Fig. 2.** The energy bands for $BaM_2$ compound, (a) $BaRh_2$, (b) $BaPd_2$ and (c) $BaPt_2$.

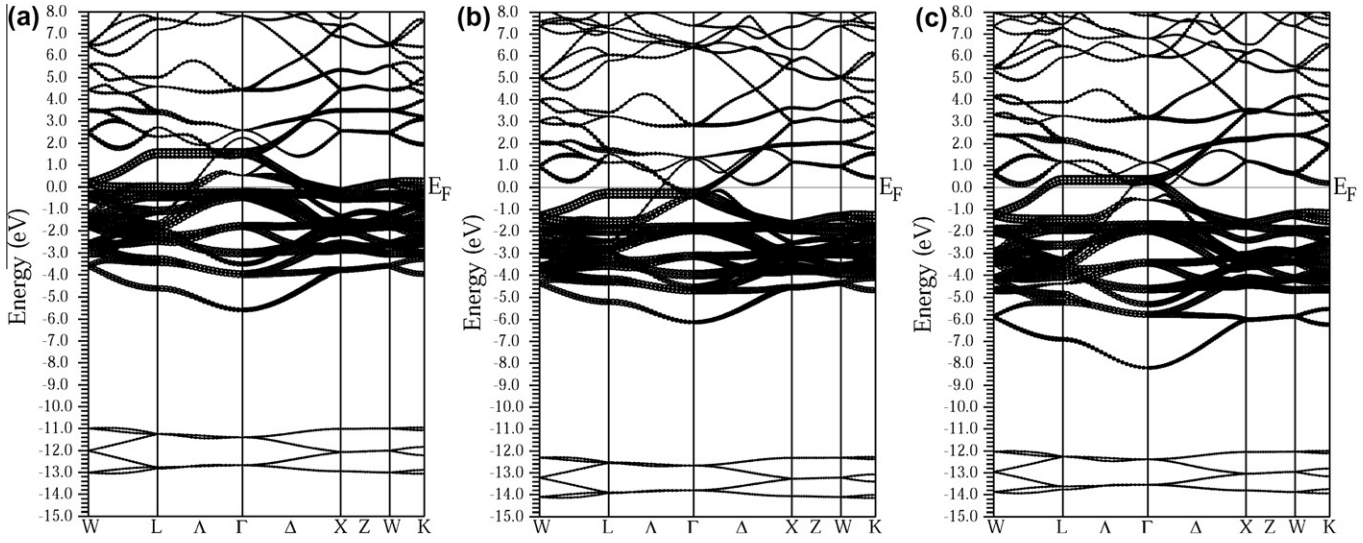


**Fig. 3.** Band structure of $BaM_2$ compounds showing *d*-character bands, (a) $BaRh_2$, (b) $BaPd_2$ and (c) $BaPt_2$.

cally favorable from the point of view of thermodynamics, and this stable structure is the most likely to be formed during experiments.

The cohesive energy is a measure of the strength of the forces that bind atoms together in the solid state and is descriptive in studying the phase stability. The cohesive energy $E_{coh}^{BaM_2}$ of $BaM_2$ is defined as the total energy of the constituent atoms minus the total energy of the compound [20]:

$$E_{coh}^{BaM_2} = \frac{[xE_{atom}^{Ba} + yE_{atom}^{M}] - E_{total}^{BaM_2}}{x+y} \Rightarrow E_{coh}^{BaM_2} = \frac{[2E_{atom}^{Ba} + 4E_{atom}^{M}] - E_{total}^{BaM_2}}{6} \quad (\text{with M} = \text{Rh, Pd, Pt.}) \tag{2}$$

where $E_{coh}$ is the total energy of the unit cell used in the present calculation, $x$ and $y$ are the numbers of Ba and (Rh, Pd, Pt) atoms in unit cell, respectively. $E_{total}^{BaM_2}$ refers to the total energy of C15-type $BaM_2$ in the equilibrium configuration and $E_{atom}^{Ba}, E_{atom}^{M}$ are the isolated atomic energies of the pure constituents. The calculated cohesive energies are presented in Table 1.

The computed cohesive energies are 6.101 eV/atom, 4.774 eV/atom and 6.512 eV/atom for $BaRh_2$, $BaPd_2$ and $BaPt_2$, respectively.

### 3.2. Electronic properties

#### 3.2.1. Band structure

The calculated energy band structure, at equilibrium lattice parameters, for $BaM_2$ along the high symmetry directions in the Brillouin zone is shown in Fig. 2a–c. The band profiles are quite similar (with slight differences) for the three studied compounds. It can be assessed from Fig. 2a–c that there is no gap at the Fermi level $E_F$ in which vicinity it exists an overlapping of valence and conduction bands. The metallicity of these three compounds $BaRh_2$, $BaPd_2$ and $BaPt_2$ is confirmed by their band structures.

We have reported additional calculations of the band structure of $BaM_2$ compounds Fig. 3a–c, showing *d*-character bands of Rh, Pd, and Pt in character plotting mode in order to make a better comparison. One clearly sees some very flat bands of mostly *d* character near the Fermi level which, are dominated Pd 4*d* and Pt 5*d* orbitals.

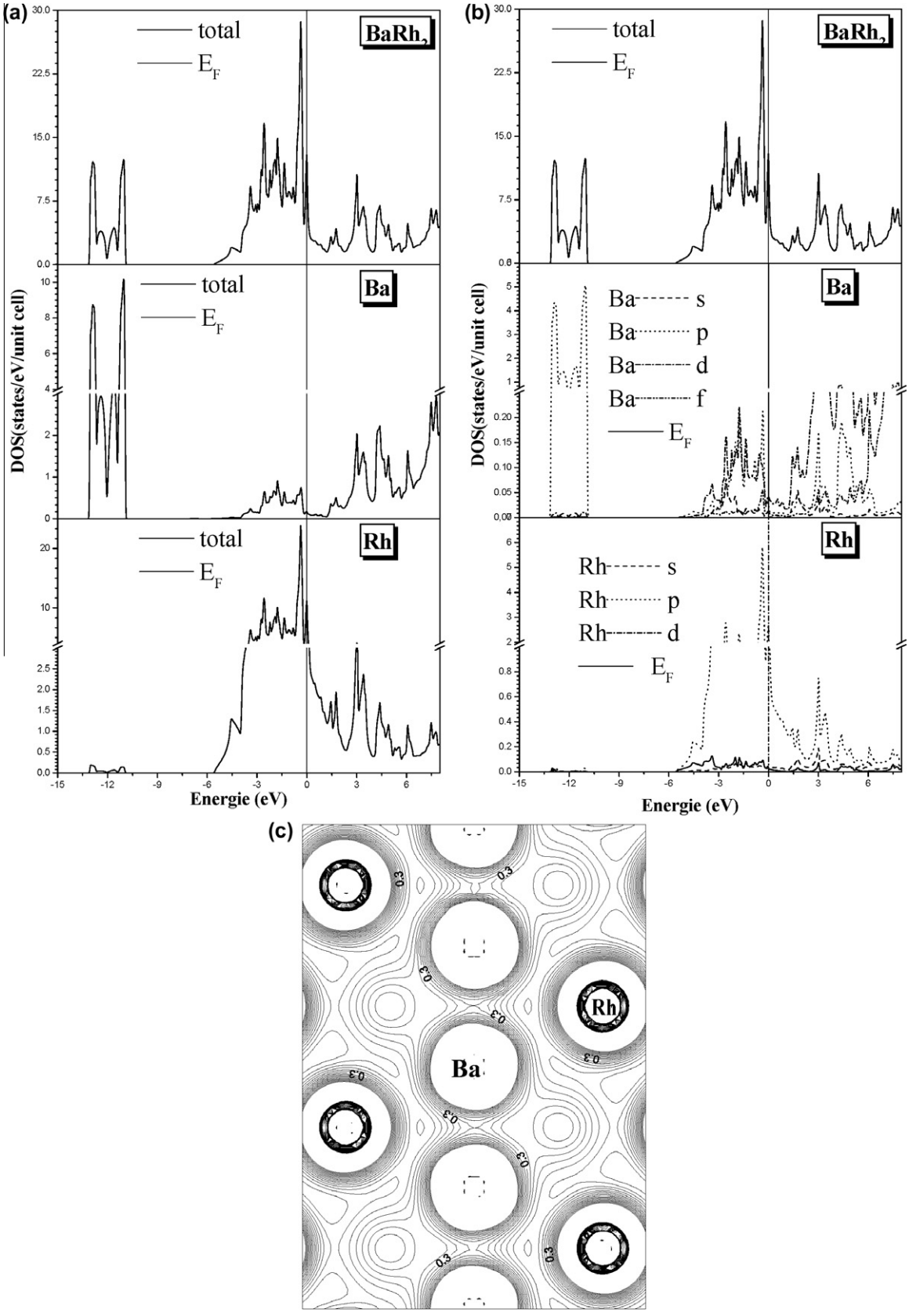


**Fig. 4.** (a) Total electronic density of states of $BaRh_2$. (b) Partial electronic density of states for C15-$BaRh_2$. (c) Distribution of bonding charge density in the (1 1 0) plane of C15-$BaRh_2$.

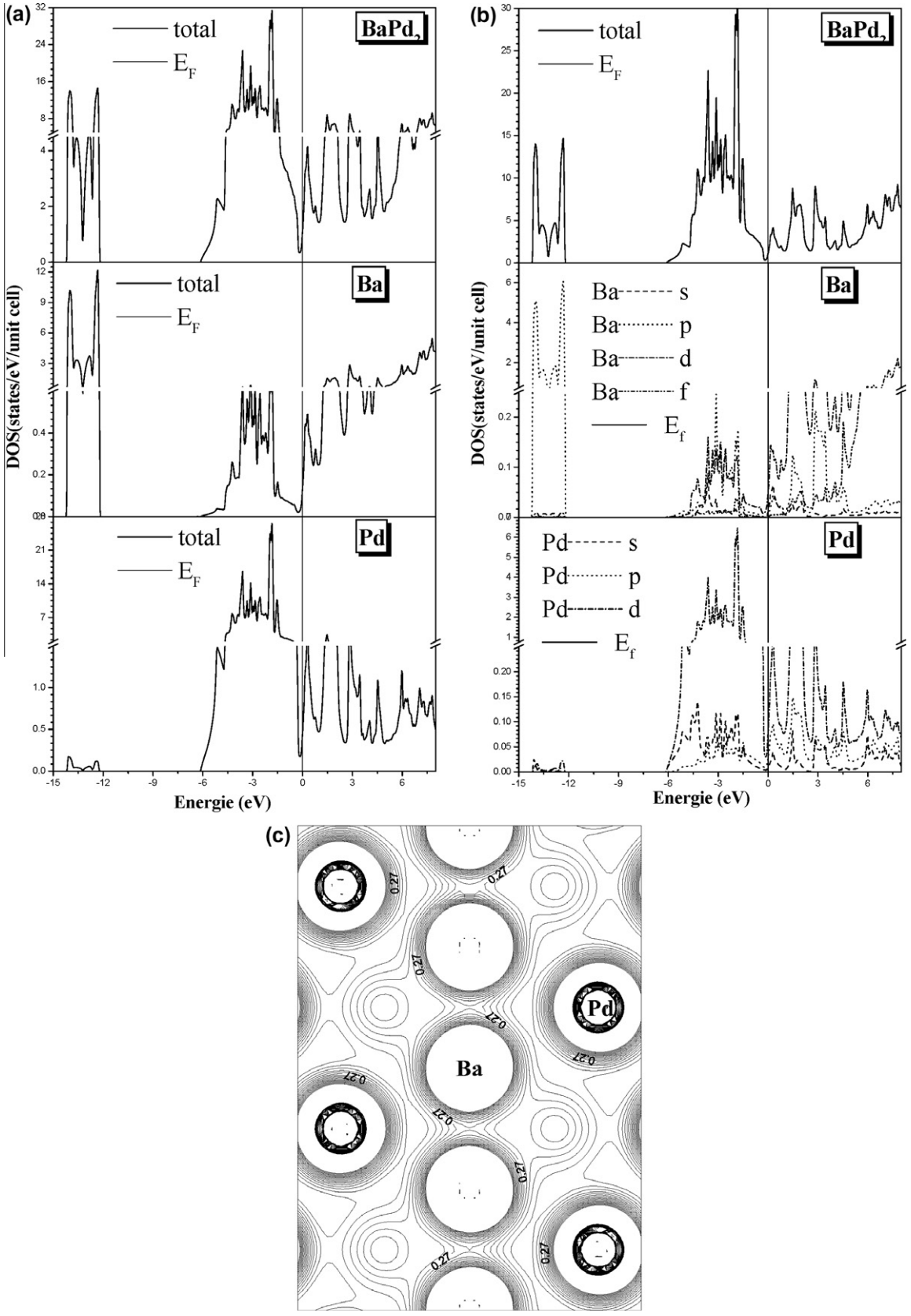


**Fig. 5.** (a) Total electronic density of states of $BaPd_2$. (b) Partial electronic density of states for C15-$BaPd_2$. (c) Distribution of bonding charge density in the (1 1 0) plane of C15-$BaPd_2$.

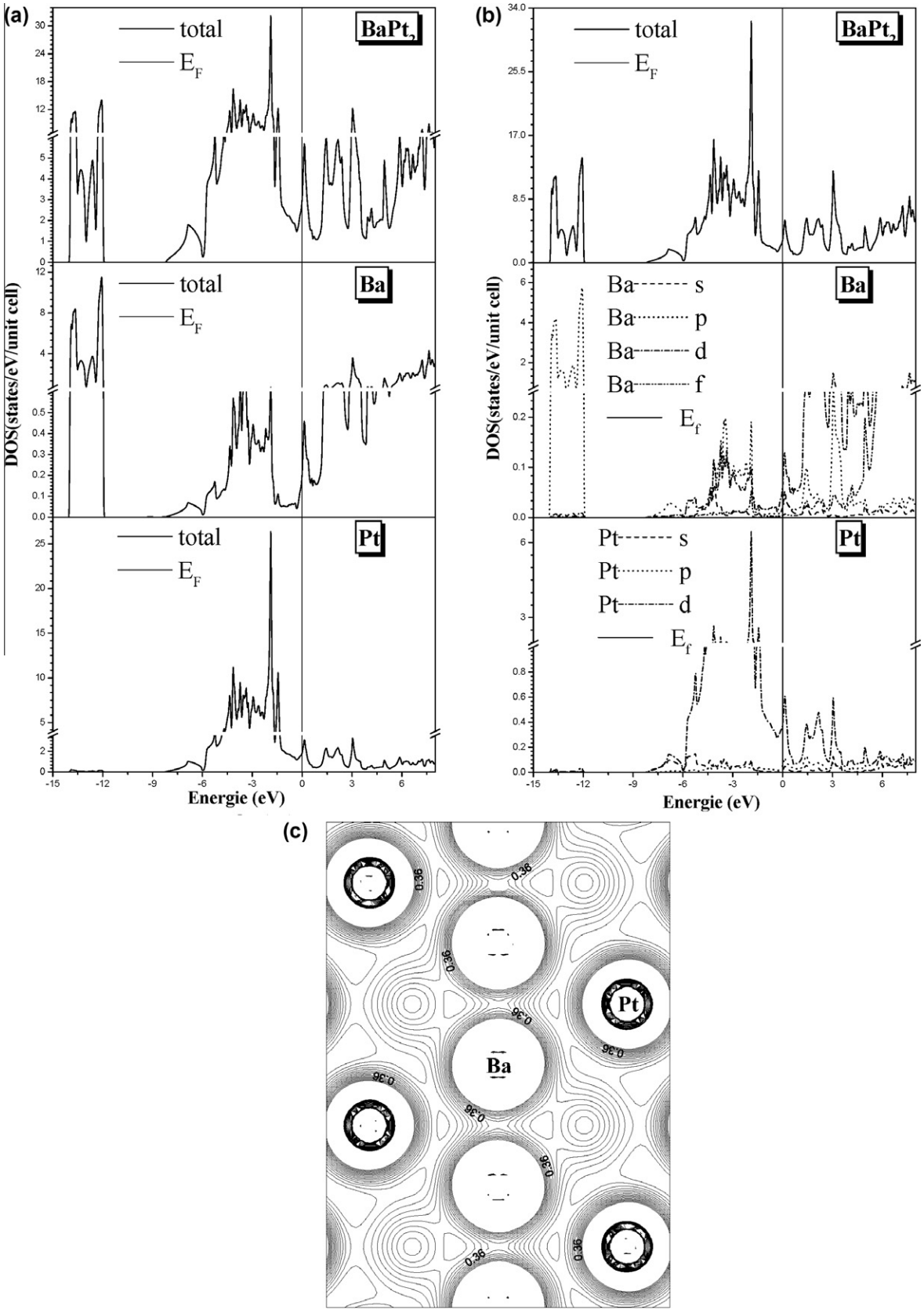


**Fig. 6.** (a) Total electronic density of states of $BaPt_2$. (b) Partial electronic density of states for C15-$BaPt_2$. (c) Distribution of bonding charge density in the (1 1 0) plane of C15-$BaPt_2$.

**Table 2**
The calculated elastic constants, bulk modulus ($B$), Young's modulus ($E$), shear modulus ($G$, $G_V$, $G_R$), Poisson's ratio and anisotropic ratio ($A$) of the C15-$BaM_2$.

| | $C_{11}$ (GPa) | $C_{12}$ (GPa) | $C_{44}$ (GPa) | $B$ (GPa) | $E$ (GPa) | $G_V$ (GPa) | $G_R$ (GPa) | $G$ (GPa) | $\upsilon$ | $A$ |
|---|---|---|---|---|---|---|---|---|---|---|
| $BaRh_2$ | 158.448 | 113.323 | 35.079 | 128.365 | 81.943 | 30.083 | 28.716 | 29.399 | 0.394 | 1.56 |
| $BaPd_2$ | 137.015 | 91.617 | 46.203 | 106.750 | 95.447 | 36.801 | 32.671 | 34.736 | 0.353 | 2.04 |
| $BaPt_2$ | 198.768 | 112.024 | 60.637 | 140.939 | 141.336 | 53.731 | 52.308 | 53.020 | 0.333 | 1.40 |

The flat bands are well separated from other bands along Γ-L direction for the compounds.

*3.2.2. Electronic densities of states (DOS) and bonding charge densities*

To understand the nature of the bonding in the C15-$BaM_2$ (M = Rh, Pd, Pt) compounds, the electronic densities of states (DOS) and bonding charge densities have been calculated. The Electronic density of states (total and partial) and Distribution of bonding charge density in the (1 1 0) plane of C15-$BaM_2$ is shown in Figs. 4–6.

The total and partial Densities of States (DOS) for all studied phases gives an information about the influence of electronic properties of constitutional atoms on their chemical bonding.

The similar DOS profiles have been also observed in the cases of C15-$BaRh_2$ (Fig. 4a and b), C15-$BaPd_2$ (Fig. 5a and b) and C15- $BaPt_2$ (Fig. 6a and b). We proceed from the fact that electrons with energies in the region of Fermi energy, $E_F$ play the main role in formation of chemical bonds. Comparing the total DOS for $BaM_2$ and local DOS for Ba and M (M = Rh, Pd, Pt) (see Figs. 4a, b, 5a, b and 6a, b) we conclude that electrons of M give the main contribution to conductivity of $BaM_2$ compound, we also note that there is no band gap for our compounds since the density of states has a non-zero value at the Fermi level which demonstrates the metallic character for these compounds (metallic bonding). Their total states at the Fermi level are 12.69 states/eV/unit cell, 1.18 states/eV/unit cell and 3.12 states/eV/unit cell for $BaRh_2$, $BaPd_2$ and $BaPt_2$, respectively. They reflect the differences of elements Rh, Pd, and Pt. The conductivity in $BaRh_2$ phase should be higher than in $BaPt_2$ and Conductivity in $BaPt_2$ phase should be higher than in $BaPd_2$ due to larger number of states at Fermi level (Figs. 4a, 5a and 6a). This is caused by significant contribution of d-electrons of M (M = Rh, Pd, Pt) (Figs. 4b, 5b and 6b).

Since $BaPd_2$ and $BaPt_2$ are isostructural and of similar chemical bonding, it can be expected that their properties may also be comparable. Fig. 2a,b and c show that the states corresponding to Rh 4*d*, Pd 4*d* and Pt 5*d* preserve similar features in these compounds. An important feature is the existence of a flat band in the band structure (peak in the DOS) in the vicinity of the Fermi level. One clearly sees some very flat bands around the Fermi level of mostly *d* character. Special attentions are concentrated to these flat bands near the Fermi level.

The flat band of $BaPd_2$ lies below the Fermi level near the Γ point, as shown in Fig. 2b. In $BaPt_2$ the flat band lies higher than in $BaPd_2$. In $BaPt_2$, more valence electrons are present in the unit cell. It leads to some additional occupation of bonding states near the Fermi level in $BaPt_2$. The Fermi level moves from a lower energy level to a higher-energy level with the substitution of the anionic element Rh by Pd and by Pt, which indicates that the increased extra valence electrons fill the hybridized bonding states. This band filling correspondingly increases the bulk modulus of $BaPt_2$. The electronic configuration for Rhodium is $4d^8\ 5s^1$, $5s^0\ 4d^{10}$ for palladium, and $4f^{14}\ 5d^9\ 6s^1$ for Platinum. The electronic configuration for palladium, Pd ($Z$ = 46). Palladium is a special case, where one can argue that the filled 4*d* subshell has lower energy than $5s^2\ 4d^8$, or $5s^1\ 4d^9$. The band filling correspondingly decreases the bulk modulus of $BaPd_2$.

The details of the peak structures and the relative heights of the peaks in the DOS are rather similar. Distinctive differences are traced to the features near the Fermi level. In $BaRh_2$ and $BaPd_2$, the Fermi level falls near a pronounced peaks, whereas it occurs on the low-energy side of a peak in the DOS for $BaPt_2$.

The Fermi level separates the fully occupied bonding states and unoccupied antibonding states for Pt and Pd. The bonding states are dominated by Ba-p and the state near to the Fermi level are dominated by M-d, while the antibonding states are dominated by Ba-d with some hybridization of M-d and Ba-f with some hybridization of Ba-d should lead to covalent bonding in $BaM_2$.

This showed a strong covalent bonding between Ba–Ba atoms and a metallic bonding between Ba–M atoms (see Figs. 4b, 5b and 6b).

In order to further explore the bonding characteristics in the $BaM_2$ (M = Rh, Pd and Pt) compounds, the charge density maps of the (1 1 0) plane are theoretically calculated as shown in Figs. 4c, 5c and 6c, where the contour lines of the higher density regions are omitted. The contour lines are plotted from 0 to 0.6 e/Å$^3$ with 0.03 e/Å$^3$ intervals. In the C15 structure of $BaM_2$ compounds, Ba atoms occupy the diamond-like lattice and M atoms are located at tetrahedral sites. The (1 1 0) plane bisects the M tetrahedral in $BaM_2$ compounds. Figs. 4c, 5c and 6c shows that Ba atoms are almost spherical, but M atoms are a little deformed. The obvious overlap of electron densities between M–M indicates a covalent bonding between them. In contrast to the M–M bonding, there is no overlap of electron densities around Ba atoms. The almost uniform electron distribution around Ba atoms is like a metallic bonding and can be well described by the nearly free electron model. The height of charge density at the bond midpoint between M–M was found to be 0.30 e/Å$^3$ for Rh–Rh, 0.27 e/Å$^3$ for Pd–Pd and 0.36 e/Å$^3$ for Pt–Pt, whereas the height of charge density at the bond midpoint between Ba–M is almost the same 0.15 e/Å$^3$. It could be assumed that the bonding between Ba–M is much weaker than that between M–M in the $BaM_2$ compounds. This could be explained from the point of view of the C15 Laves phases structure. Compared with the atomic distance between the next nearest Ba–M and M–M atoms, the M–M covalent bonding is thus stronger than that between the Ba–M atoms which is a mainly metallic bonding in $BaM_2$. While the electro-negativities of Ba and M atoms differ significantly 0.9 and 2.2, respectively, according to the scale of Pauling electronegativity confirms the ionic character in the bonding between the element Ba and M.

*3.3. Elastic properties*

The elastic properties play an important role in providing valuable information about the binding characteristic between adjacent atomic planes. Anisotropic characters of binding and structural stability are usually defined by the elastic constants $C_{ij}$. These constants have been often related to the shear modulus G and Young's modulus Y. Ab initio calculation of the elastic constants requires precise methods. For obtaining the elastic constants from their known structure a popular approach [21,22], which is based on the analysis of the changes in calculated total energy values resulting from changes in the strain, is used. A cubic structure is characterized by three independent elastic constants, namely $C_{11}$, $C_{12}$ and $C_{44}$. The obtained elastic constant values for $BaRh_2$, $BaPd_2$ and $BaPt_2$ are given in Table 2. Note that the elastic constants of these compounds were not measured experimentally.

The values of the elastic constants decrease in going from $BaPt_2$ to $BaRh_2$ to $BaPd_2$, this indicates that $BaPt_2$ is rigid than $BaRh_2$, and $BaRh_2$ and is rigid than $BaPd_2$.Based on these results, we find that the stability criteria [23,24]:

$C11 - C12 > 0, C11 > 0, C44 > 0, (C11 + 2C12) > 0$ are satisfied for these compounds, and therefore these compounds are elastically stable.

It may be noted that the value of B (bulk modulus) calculated from the elastic constants has nearly the same value as that obtained from by fitting the total energy versus volume according to the Murnaghan's equation of state [18]. This gives us a good estimate of the precision and accuracy of the elastic constants of $BaRh_2$, $BaPd_2$ and $BaPt_2$.

From the elastic constants we obtain the anisotropy parameter A given by the expression:

$$A = \frac{2C_{44}}{C_{11} - C_{12}} \tag{3}$$

For an isotropic crystal A is 1, while another value greater than or less than 1 means that it is an anisotropic crystal. According to the values of A listed in Table 2, $BaRh_2$, $BaPd_2$ and $BaPt_2$ are anisotropic.We can get other important elastic properties for various technological applications:

$\upsilon$: Poisson's ratio that characterizes the traction of the solid perpendicular to the direction of the force applied.

$E$: Young's modulus which measures the strength of the solid to change its length.

$G$: the shear modulus which measures the resistance to movement of the slip planes inside the solid with planes parallel to them.

From the following equations [25]:

$$\upsilon = \frac{1}{2}\left[\frac{(B - \frac{2}{3}G)}{(B + \frac{1}{3}G)}\right] \tag{4}$$

$$E = \frac{9GB}{G + 3B} \tag{5}$$

$$B = \frac{1}{3}(C_{11} + 2C_{12}) \tag{6}$$

As $B$ is the bulk modulus which measures the resistance to volume changes in solids and thus gives an estimate of the elastic response of a material to hydrostatic pressure. There are two methods for calculating the shear modulus of a material isotropic monophasic polycrystalline isotropic and statistically defined by Voigt in 1928 [26] and Reuss in 1929 [27].Voigt method is the application of a uniform stress ($\sigma$) on the cell, and gives the shear modulus as a function of elastic constants:

$$G_V = \frac{1}{5}(C_{11} - C_{12} + 3C_{44}) \text{ (For cubic system)}. \tag{7}$$

Reuss method is the application of a uniform strain ($\varepsilon$) of the cell, and gives the shear modulus as a function of elastic constants:

$$\frac{5}{G_R} = \frac{4}{C_{11} - C_{12}} + \frac{3}{C_{44}} \tag{8}$$

The shear modulus $G$ is given by the arithmetic mean of $G_V$ and $G_R$:

$$G = \frac{1}{2}(G_V + G_R) \tag{9}$$

Our results on Young's modulus ($E$), the shear modulus ($G$) and Poisson's ratio ($\nu$) of the three compounds using LDA are listed in Table 2. Based on this result $E$ and $G$ for $BaPt_2$ are larger than $BaPd_2$ and $E$ and $G$ for $BaPd_2$ are larger than $BaRh_2$, so $BaPt_2$ is more resistant to tensile and shear strength that $BaPd_2$ and $BaRh_2$.

## 4. Conclusion

In this work we have used first-principles calculations using the FLAPW method within the LDA to describe the electronic structure and elastic properties of a series of C15 binary $AB_2$ type Laves phases $BaRh_2$, $BaPd_2$ and $BaPt_2$. Their lattice constants, formation and cohesive energy, and elastic properties have been calculated, the calculated equilibrium lattice constants are in good agreement with the experimental values available but for the other properties there are no experimental or theoretical data in literature for compared. The calculated elastic constants satisfy the criteria of mechanical stability of a cubic phase.

Analysis of total and partial DOS for all studied Laves phases allowed getting information about the nature of chemical bonding in these compounds. Promoted *f*-electrons of Ba participate in covalent bonding which is determined by a superposition of *d*- and f-states of Ba electrons. Promoted *d*-electrons of M play partly a role of conductive electrons and consequently participate in metallic bonding. Electro-negativities of Ba and M atoms differ significantly (0.9 and 2.2 accordingly). Thus the ionic component in the bonding is significant. On the other hand, there is virtually no covalency between Ba–M atoms, although $BaM_2$ are called intermetallic compounds. In the interatomic region, the electrons are distributed evenly like a metallic bond.

## References


[1] (a) Friauf JB. J Am Chem Soc 1927;49:3107;
(b) Friauf JB. Phys Rev 1927;29:34.
[2] Laves F, Witte H. Metallwirt 1935;14:645.
[3] Hilscher G. J Magn Magn Mater 1982;27:31.
[4] Chen X-Q, Wolf W, Podloucky R, Marsman PRogletM. Phys Rev B 2005;72:054440.
[5] Palm SMilenkovicetM. Intermetallics 2008;16:1212.
[6] Hishinuma Y, Kikuchi A, Iijima Y, Yoshida Y, Takeuchi T, Nishimura A, Inoue K. Fusion Eng Des 2006;81:975.
[7] Saini NL, Agrestini S, Amato E, Filippi M, Di Castro D, Bianconi A, Manfrinetti P, Palenzona A, Marcelli A. Phys Rev B 2004;70:094509.
[8] Young K, Fetcenko MA, Ouchi T, Koch FLietJ. J Alloy Comp 2009;469:406.
[9] Liu X, Asano K, Akiba NTerashitaetE. Int J Hydrogen Energ 2009;34:1472.
[10] Hong S, Lu CL. Phys Rev B 2002;66:94109.
[11] (a) Theory of Alloy Pases, American Society of Metallurgists, Cleveland; 1956.;
(b) Westbrook JH, editor. Intermetallic Compounds. New York: Wiley; 1967;
(c) Pearson WB. The Crystal Chemistry and Physics of Metals and Alloys. New York: Wiley; 1972;
(d) Villars P, Calvert etLD. Pearson's handbook of crystallographic data for intermetallic phases the materials information society. 2nd ed. Materials Park; 1991.
[12] Blaha P, Schwarz K, Madsen GKH, Kvasnicka D, Luitz J. In: Schwarz K, editors. WIEN2k: an augmented plane wave + local orbitals program for calculating crystal properties. Austria: Technische Universität Wien; 2001.
[13] Blaha P, Schwarz K, Luitz J, WIEN97: a full potential wave package for calculating crystal properties, Austria: Vinna University of Technology; 2001.
[14] Perdew JP, Wang Y. Phys Rev B 1992;45:13244.
[15] Kohn W, Sham LJ. Phys Rev 1965;140:A1133.
[16] Monkhorst HJ, Pack JD. Phys Rev B 1976;13:5188.
[17] Paolasini L, Hennion B, Panchula A, Myers K, Canfield P. Phys Rev B 1998;58:2125.
[18] Murnaghan FD. Proc Natl Acad Sci USA 1944;30:5390.
[19] Wood Elizabeth A, Compton Vera B. Acta Cryst 1958;11:429.
[20] Huang ZW, Zhao YH, Hou H, Han PD. Physica B 2012.
[21] Mehl MJ. Phys Rev B 1993;47:2493.
[22] Khenata R, Bouhemadou A, Reshak AH, Ahmed R, Bouhafs B, Rached D, Al Douri Y, Rérat M. Phys Rev B 2007;75:195131.
[23] Born M, Proc Cambridge Philos Soc 1940;36:160.
[24] Born M, Huang K, Dynamical theory of crystal lattices, édité par, Oxford: Clarendon; 1956.
[25] Schreiber E, Anderson OL, Elastic Constants N Soga, Measurements Their. New York: McGraw-Hill; 1973.
[26] Voigt W, Lehrbuch der Kristallphysik, édité par Taubner, Leipzig; 1929.
[27] Reuss A, Angew Z. Math Mech 1929;9:49.